Effect of Wind and Temperature Gradients on Received Acoustic Energy *

Richard K. Brienzo
Lincoln Laboratory, Massachusetts Institute of Technology
Lexington, Massachusetts 02173

Abstract

The effect of refraction due to wind and temperature gradients on energy received from low flying aircraft is examined. A series of helicopter and jet flyby's were recorded with a microphone array on two separate days, each with distinctly different meteorological conditions. Energy in the 100-200 Hertz band is shown as a function of aircraft range from the array, and compared with the output of the Fast Field Program.

I. Introduction

This paper examines the effect of wind and temperature gradients on energy received at a microphone array from a series of aircraft flyby's. Of interest is the energy contained between 100 and 200 Hertz, the frequency band used in our acoustic detection and tracking algorithms.

One aspect of this work is to estimate our ability to detect and track low flying aircraft, or conversely, to assess the vulnerability of aircraft to acoustic detection and tracking. Propagation characteristics, which are largely influenced by wind and temperature gradients, must be taken into account if we are to make accurate predictions.

To illustrate the impact that wind and temperature gradients can have, received energy as a function of aircraft range has been calculated from aircraft flyby's on two separate days, each with distinctly different meteorological conditions. Sound speed profiles, derived from wind and temperature data collected during the experiments, are used to generate ray plots. Visualization of the ray paths helps to explain features seen in the experimental data.

To predict detection range or tracking ability for a given set of meteorological parameters, we must estimate acoustic energy as a function of distance from the source. To this end, the output of a propagation model, the Fast Field Program, is compared to the experimental results.

* This work was sponsored by the Department of the Air Force.

II. Experiment

Aircraft flyby's, depicted in Figure 1, were recorded on two different days (designated as Day 1 and Day 2). Results presented here are from a helicopter on Day 1, and a jet aircraft on Day 2. Both aircraft flew in a straight line at a constant altitude past a nine element microphone array. Ground truth TSPI (Time SPace Information) of the aircraft's position and velocity, corrected for acoustic propagation time, was also recorded during each flyby. Details are given in Table 1.

Array data were sampled at 2048 samples/second during the experiment and recorded directly to magnetic tape. The array consisted of nine GenRad 1962-P42 microphones with standard Sennheiser windscreens. Microphones were placed in notched wooden blocks on the ground in a tri-delta configuration (reference 1). The array was used with a wideband direction finding program (reference 2) to aid in determining whether received energy was signal from the aircraft, or noise. This is discussed further in Section IV.

Meteorological data (temperature, wind speed and direction, and relative humidity) were recorded to a height of 300 meters before and after the experiment using a tethered balloon. These parameters were also recorded on the ground throughout both experiments. Meteorological data were stored every 10 seconds during the experiment. The wind was from the South (190 degrees) on Day 1, and from the North (15 degrees) on Day 2. Headings of 345 and 165 degrees put the aircraft approximately into the wind, or with the wind.

The helicopter was louder when it was inbound to the array, so only incoming portions of the helicopter data are analyzed. There were two runs incoming from the North (345 degrees), and two runs incoming from the South (165 degrees). The closest point of approach (CPA) from each direction was 90 and 230 meters.

The jet was louder outbound from the array, so only outgoing portions of those runs are used. Three runs outgoing to the North (345 degrees), and three runs outgoing to the South (165 degrees) are analyzed. The CPA for these runs varied from 140 meters to 716 meters.

III. Data

Array data

The array time series for one of the helicopter runs at its CPA is shown in Figure 2a. This same time series is displayed in Figure 2b after bandpass filtering between 100 and 200 Hertz. The spectra from two of the channels are shown in Figure 3. These spectra show the strong harmonic structure that is typical for helicopters.

Array time series for the jet are shown in Figures 4a and 4b. The jet spectrum from two of the channels are shown in Figure 5. These figures illustrate the broadband spectra that is typical of jets.

The drop in power level in both Figures 3 and 5 at about 750 Hertz is due to the antialiasing filter. A rise in energy below 50 Hertz in the spectra of Figure 5 is due to wind noise.

Environmental data

Meteorological data collected from a tethersonde was used to calculate sound speed as a function of height. Data taken during one of the balloon raisings on Day 1 is shown in Figure 6. There was a normal temperature lapse above 50 meters, with the wind out of the South. Sound speed profiles for Day 1 at 345 degrees (looking North of the array) and 165 degrees (looking South of the array) are shown in Figure 7.

On Day 2, the wind was from the North (Figure 8). The wind speed initially increased up to 70 meters, then decreased with height, up to 300 meters. This unusual wind profile, along with a temperature inversion, led to the sound speed profile in figure 9.

IV. Analysis

Energy as a function of range

Received energy is calculated for each one-second segment (2048 points) of the array time series. This corresponds to a spatial average of about 30 meters for the helicopter, and 240 meters for the jet. The power spectrum for each channel is first calculated using a Hanning window and 2048 point fft's. After integrating the power spectra between 100 and 200 Hertz, the values for all channels are averaged. The level calculated for that one-second segment is then matched to the corresponding TSPI range, yielding energy received at the array when the aircraft was at that particular range.

Separating signal from noise

It is not always clear if acoustic energy received at a microphone is signal from an aircraft, or wind noise. Whether it is signal or noise will depend upon the propagation conditions (for example, the presence of a shadow zone), the level of wind noise, and the distance from the aircraft to the microphone. Discriminating between signal and noise is important when comparing the output of a propagation model to experimental data; we do not want to ascribe propagation effects to our experimental data when no signal is there to model. To ensure that we were only looking at signal from the aircraft, the array time series was used with a wideband direction finding algorithm (reference 2) to classify the received energy as signal or noise.

The direction finding algorithm outputs the energy arriving along a specified number of directions. The direction from which the maximum energy arrives is the detected azimuth of the source. Energy and azimuth pairs for other directions are output in order of

decreasing received energy. For energy to be selected as signal from the aircraft, we require the detected azimuth to be close to the azimuth reported by the TSPI (ground truth) data. In addition, we require that energy coming from the direction of the detection be larger than energy coming from other directions, otherwise we are probably measuring ambient noise. All energy versus range data reported in the next section have been screened using the above criteria.

Received energy data

To help in understanding features in the received acoustic energy data, raytraces were calculated (reference 3) using the sound speed profiles from Figures 7 and 9, and are shown along with the energy versus range plots. The ray plot for the case when the helicopter was incoming from the North on Day 1 (calculated from the sound speed profile in Figure 7a) is shown in Figure 10a.

If the aircraft is considered to be at zero range and an altitude of 40 meters on the ray plot, then the number of rays intersecting the ground at any range gives an indication of the acoustic energy that would be received at that distance from the aircraft. Since the sound speed decreases with height (Figure 7a), rays leaving the aircraft bend upward, and a shadow zone is formed at about one kilometer from the source.

The received acoustic energy as a function of range for runs in which the helicopter was incoming from the North is given in Figure 10b. Each data point represents the energy averaged over one second in the 100 - 200 Hz. band. To provide a reference, a solid curve representing spherical spreading is shown along with the experimental data. As suggested by the raytrace, there is a larger decrease in received energy than predicted by spherical spreading past one kilometer, where the shadow zone begins. Note that the energy level drops significantly in the shadow zone, but does not go to zero, as ray theory predicts.

The raytrace and energy plot for runs in which the helicopter was incoming from the South are shown in Figure 11. In this case, the sound speed increased with height (Figure 7b), causing the rays to be bent downward. Energy received past about one kilometer is less than that predicted by spherical spreading since much of the energy is refracted downward at short ranges; rays are more spread out at longer ranges than would be the case for spherical spreading. Other factors, such as directivity of the source, and the ground effect, are likely to be present as well.

The raytrace (calculated from the velocity profile in Figure 9a) and energy plot for outgoing runs to the North on Day 2 (jet) are given in Figure 12. The raytrace suggests a received energy somewhat higher than indicated by spherical spreading at short ranges where the rays are refracted downward, and less received energy at longer ranges where the rays are refracted upward. Comparison of the experimental data and the spherical spreading curve shows this to be the case.

When the aircraft was South of the array, an initial decrease in sound speed up to 80 meters in height (Figure 9b) caused shallow angle downgoing rays to be bent upward,

creating a small shadow zone. Past 80 meters, there was a general increase in sound speed with increasing height, which caused the rays to be bent downward. The steep drop in received energy (Figure 13b) between one and three kilometers corresponds to the shadow zone seen in the raytrace. There is an increase in energy between four and six kilometers as rays leaving the source with an upward angle were refracted back downward.

V. Comparison with FFP

Sound speed profiles in Figures 7 and 9 were used as input to the Fast Field Program (references 4-6). As seen in Figures 14 and 15, agreement between the model output and general features in the experimental data is quite good. In particular, note that the FFP output closely models the experimental data in the shadow zones seen beyond one kilometer in Figure 14a, and between one and three kilometers in Figure 14b.

VI. Summary

Measurements of acoustic energy from a series of aircraft flyby's were presented. Features in the experimental data were explained in terms of the propagation characteristics present at the time. Sound speed profiles, from meteorological data taken during the experiment, were used as input to the Fast Field Program. The FFP was seen to provide an excellent prediction of the general features found in the experimental data. The large difference between the experimental results and simple spherical spreading emphasizes the need for accurate and detailed meteorological data.

References

1. D.P. McGinn, T.E. Landers, "AVSE Acoustic Measurement Instrumentation and Techniques", Project Report CMT-69, Lincoln Laboratory, MIT (1985).

2. S. H. Nawab, F.U. Dowla, R.T. Lacoss, "Direction Determination of Wideband Signals", IEEE ASSP-33, 1114-1122 (1985).

3. H. Weinberg, "Generic Sonar Model", NUSC Technical Document 5971D, Naval Underwater Systems Center, New London, CT (June 1985).

4. Fast Field Program (FFP), U.S. Army Construction Engineering Research Laboratory, P.O. Box 4005, Champaign, IL 61824-4005.

5. S.W. Lee, N. Bong, W.F. Richards, R. Raspet, "Impedance formulation of the fast field program for acoustic wave propagation in the atmosphere", J. Acoust. Soc. Am., 79(3), 628-634 (1986).

6. S.J. Franke, G.W. Swenson, Jr., "A Brief Tutorial on the Fast Field Program (FFP) as Applied to Sound Propagation in the Air", Applied Acoustics 27, 203-215 (1989).

Table 1.

Day	Aircraft	Heading (degrees)	Velocity (m/sec.)	Wind speed (m/sec.)	Wind direction (degrees)
1	helicopter	345/165	30	1.3	190
2	jet	345/165	240	2.9	15

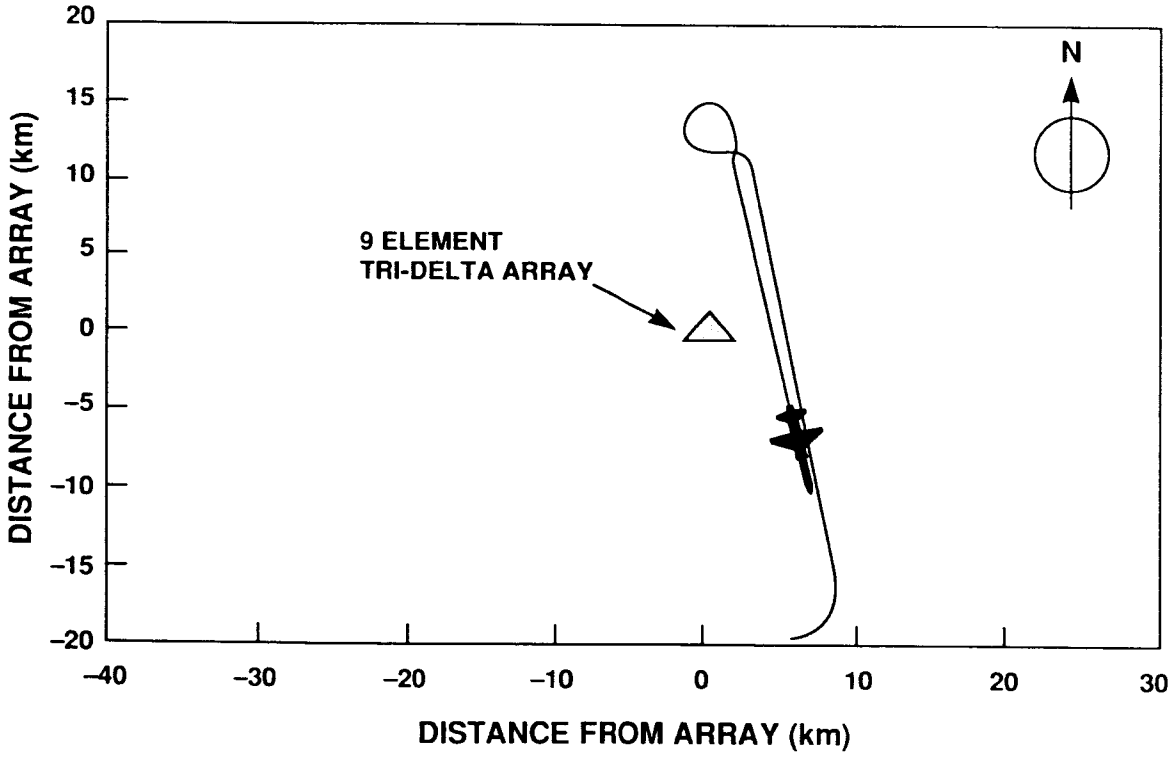

Figure 1. Aircraft flyby.

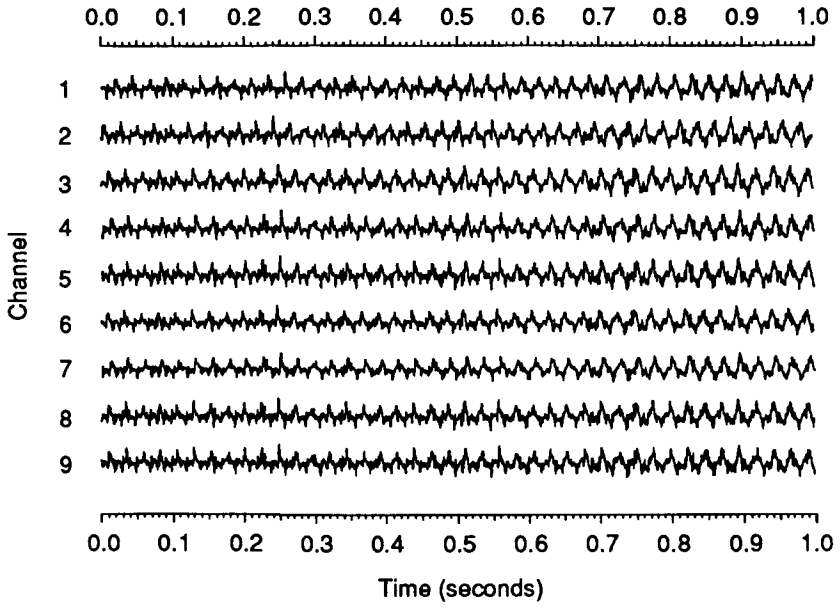

a) unfiltered time series.

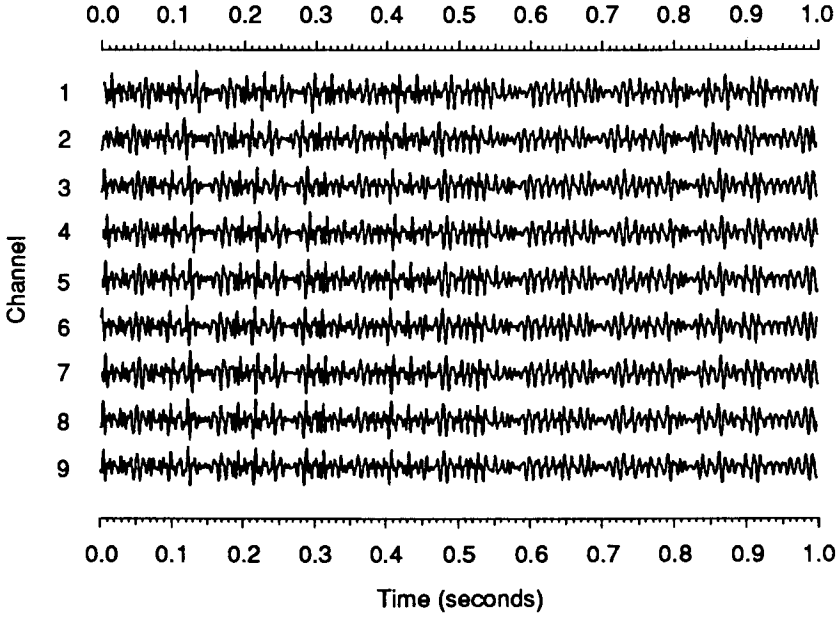

b) bandpass filtered time series [100 - 200 Hz.]

Figure 2. Helicopter time series at closest point of approach (90 meters).

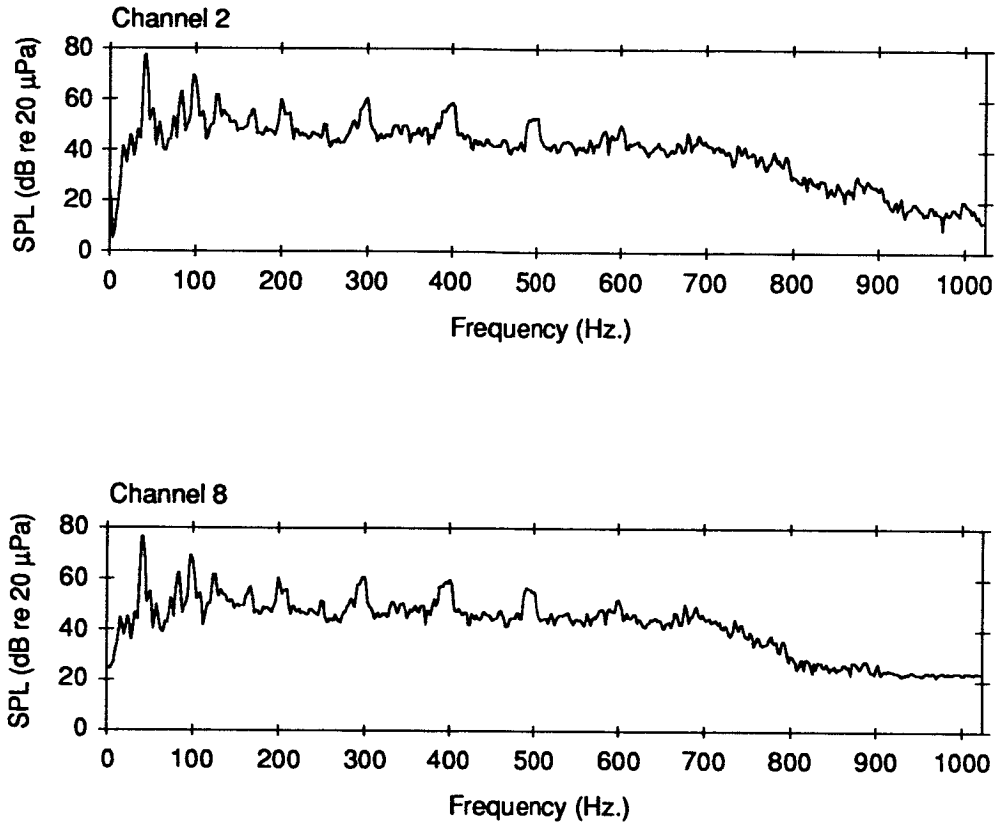

Figure 3. Helicopter spectra at closest point of approach (90 meters).

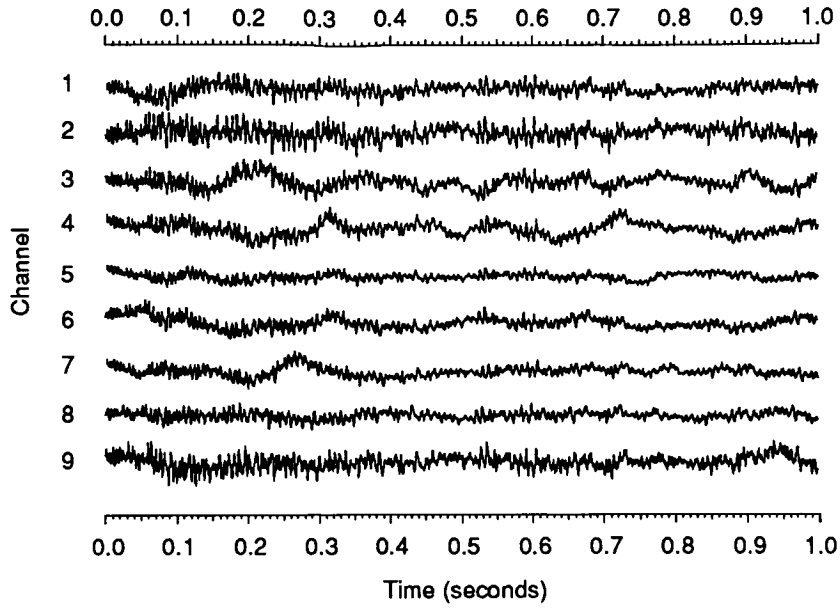

a) unfiltered time series.

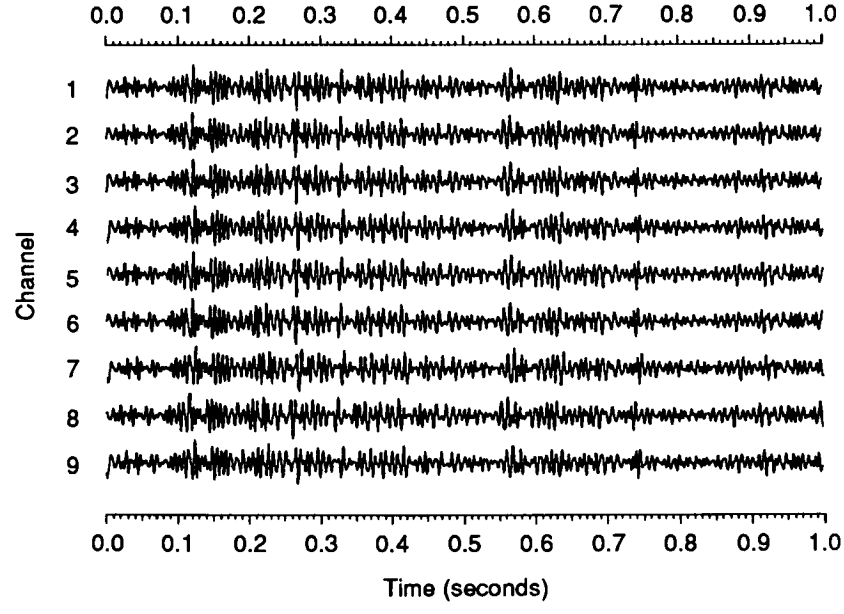

b) bandpass filtered time series [100 - 200 Hz.].

Figure 4. Jet time series at closest point of approach (716 meters).

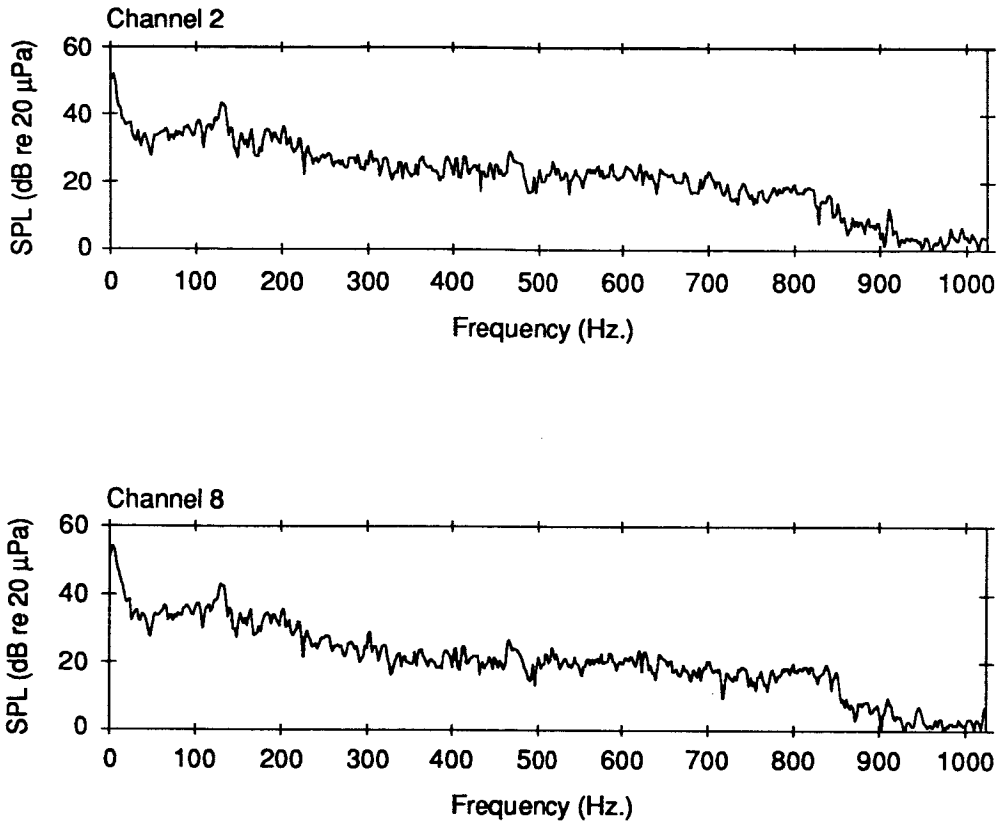

Figure 5. Jet spectra at closest point of approach (716 meters).

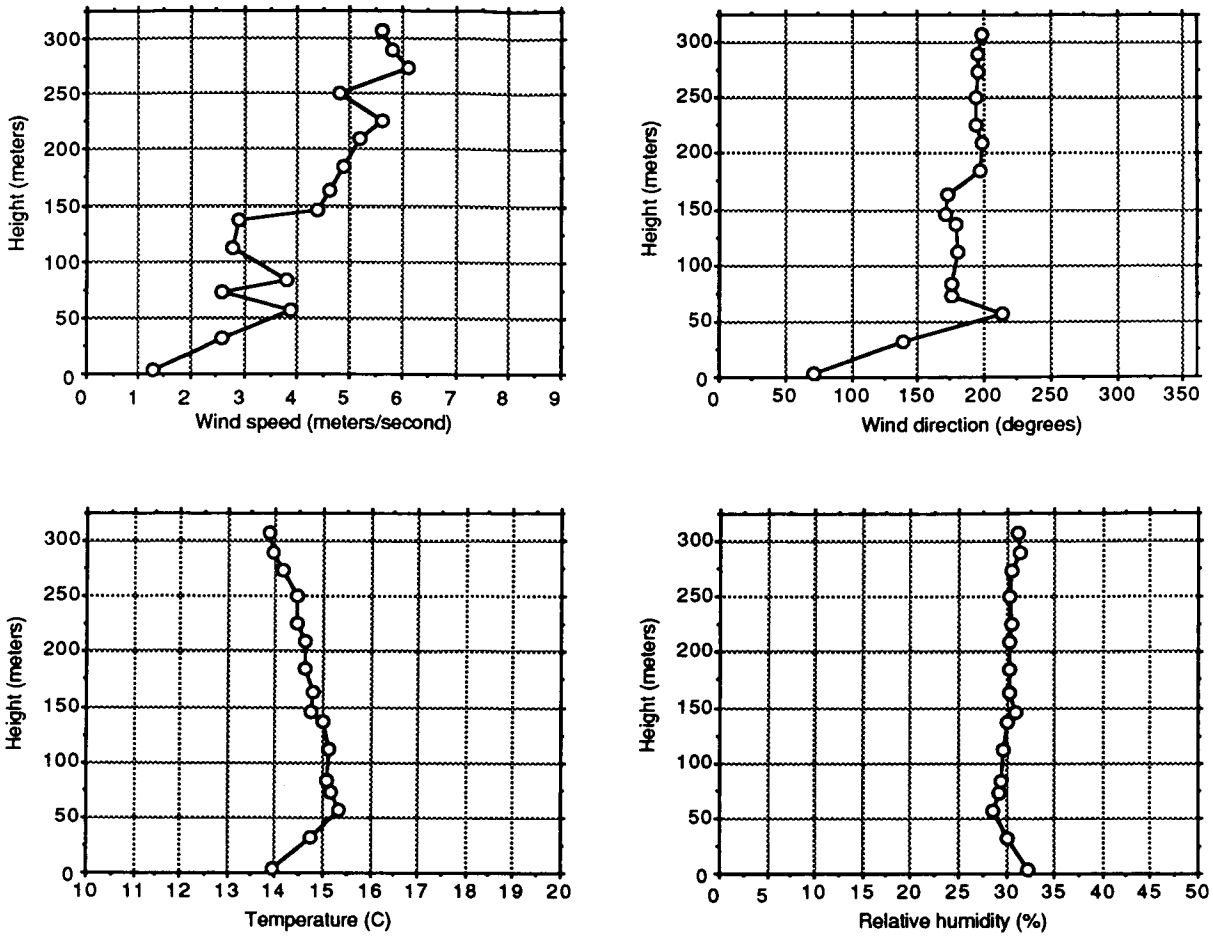

Figure 6. Day 1 meteorological data.

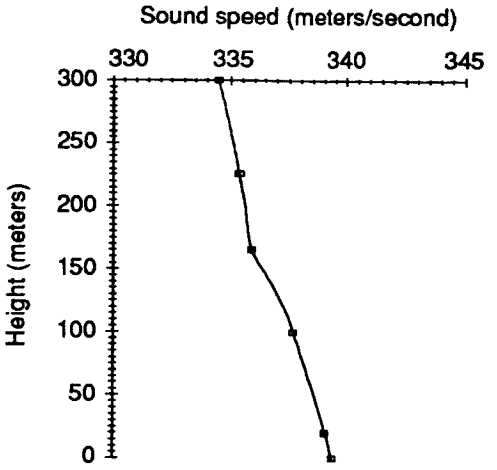

a) North of the array (345 degrees).

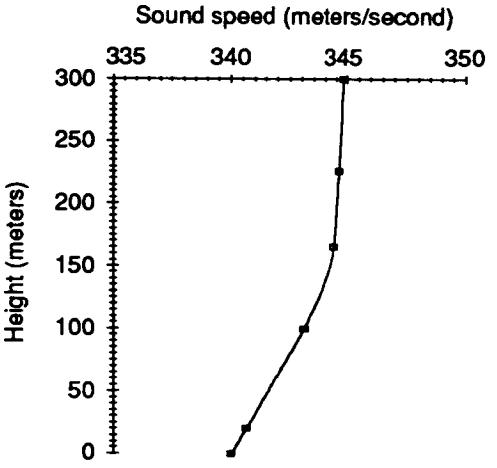

b) South of the array (165 degrees).

Figure 7. Sound speed profiles on Day 1.

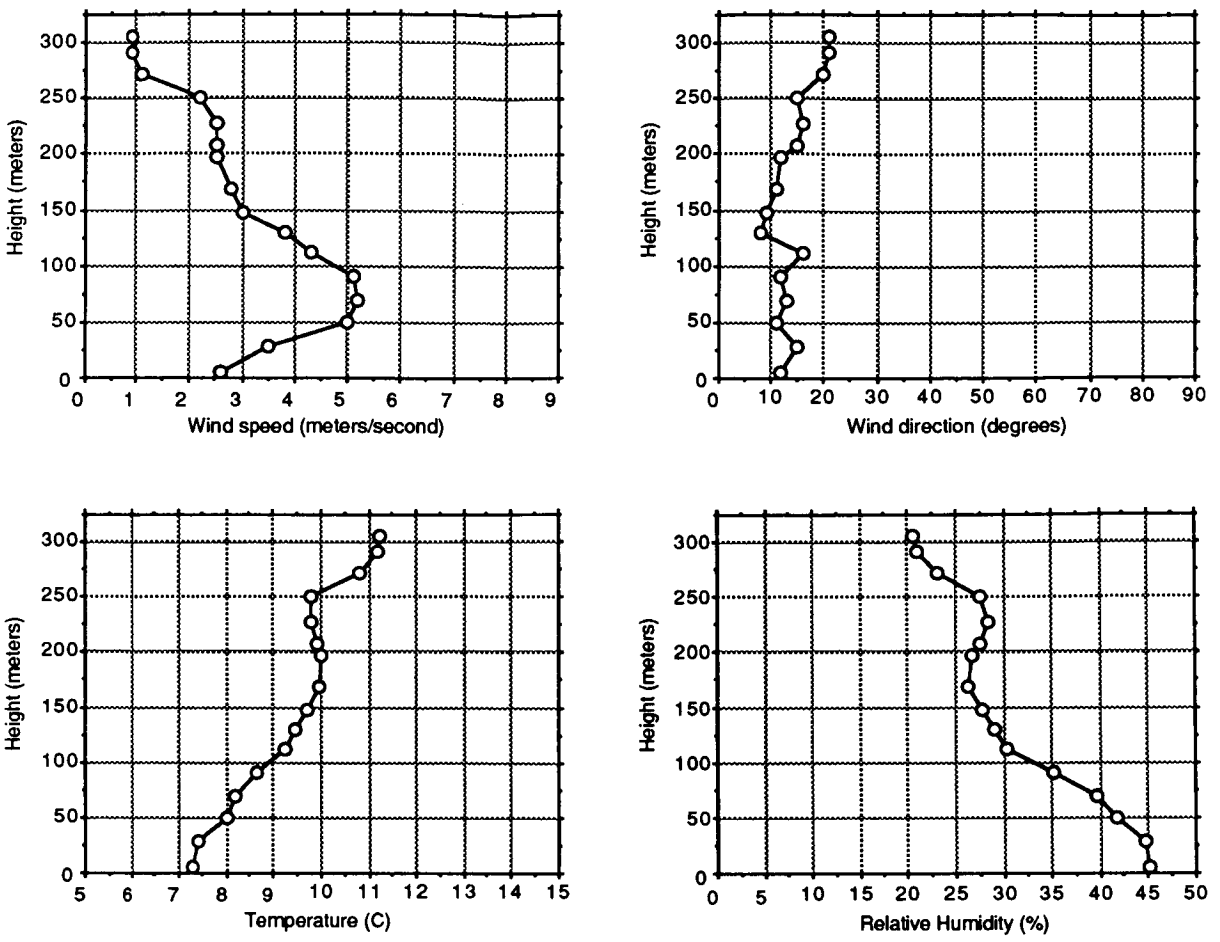

Figure 8. Day 2 meteorological data.

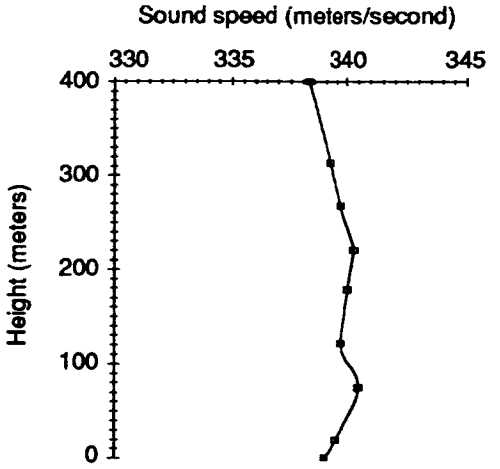

a) North of the array (345 degrees).

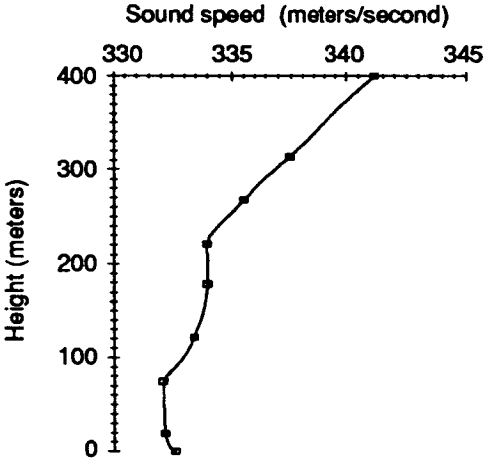

b) South of the array (165 degrees).

Figure 9. Sound speed profiles on Day 2.

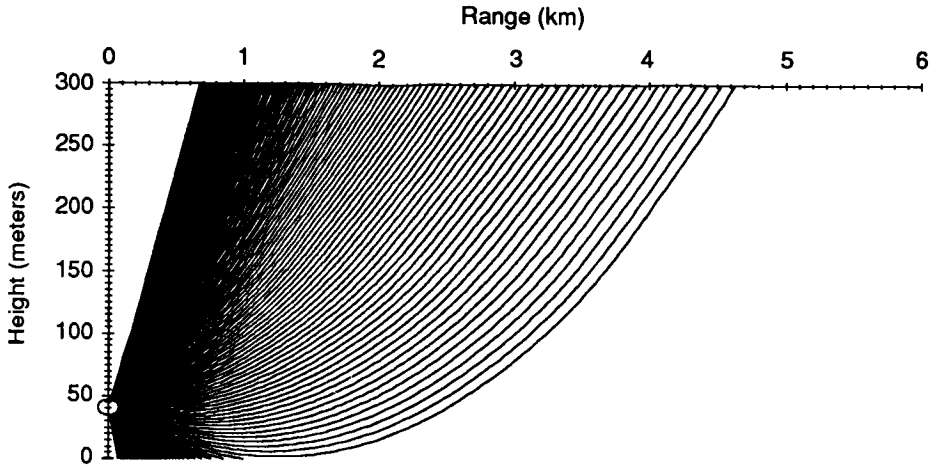

a) raytrace calculated from the velocity profile in Figure 7a.

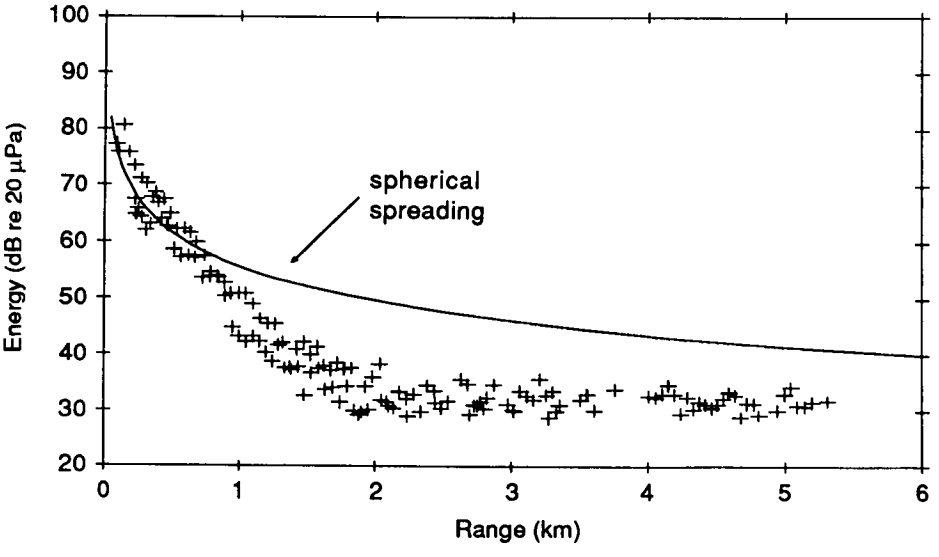

b) experimental data.

Figure 10. Helicopter incoming from the North (Day 1).

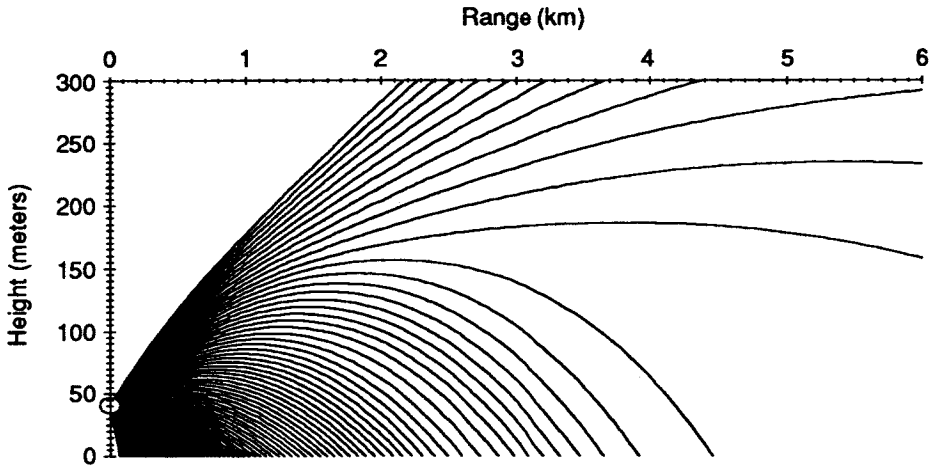

a) raytrace calculated from the velocity profile in Figure 7b.

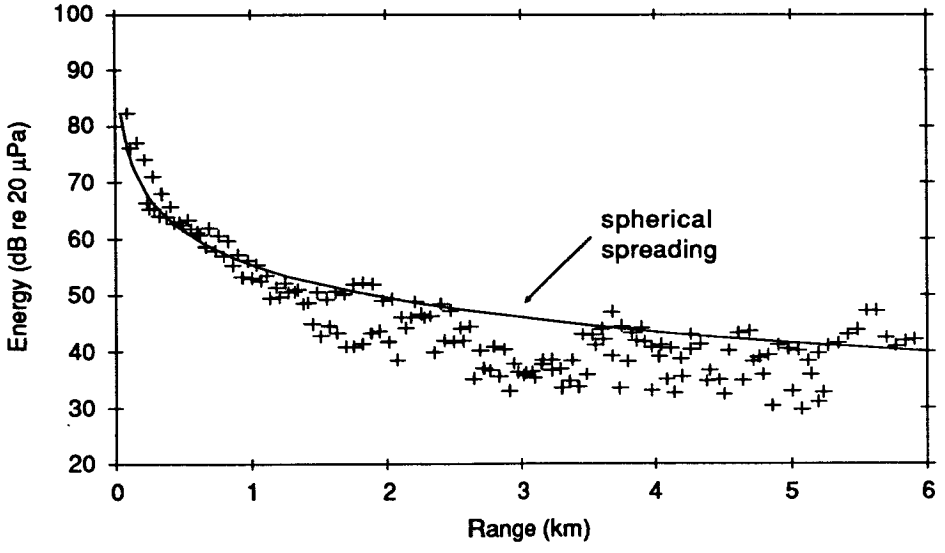

b) experimental data.

Figure 11. Helicopter incoming from the South (Day 1).

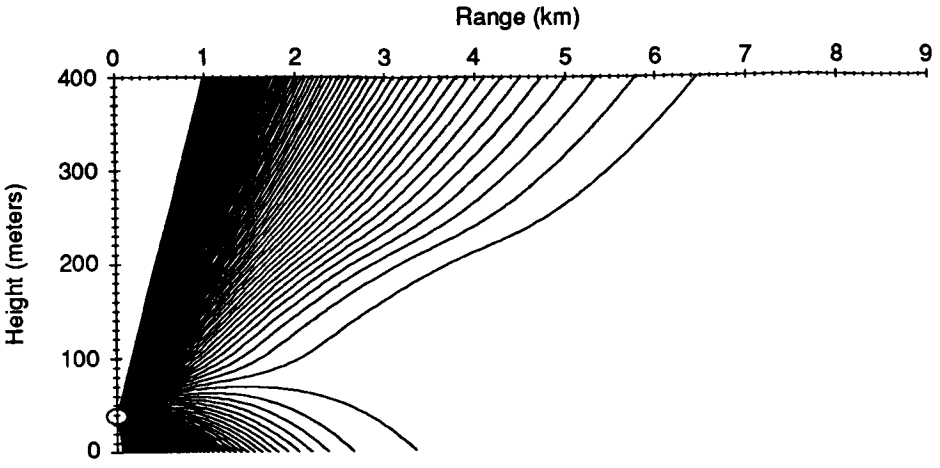

a) raytrace calculated from the velocity profile in Figure 9a.

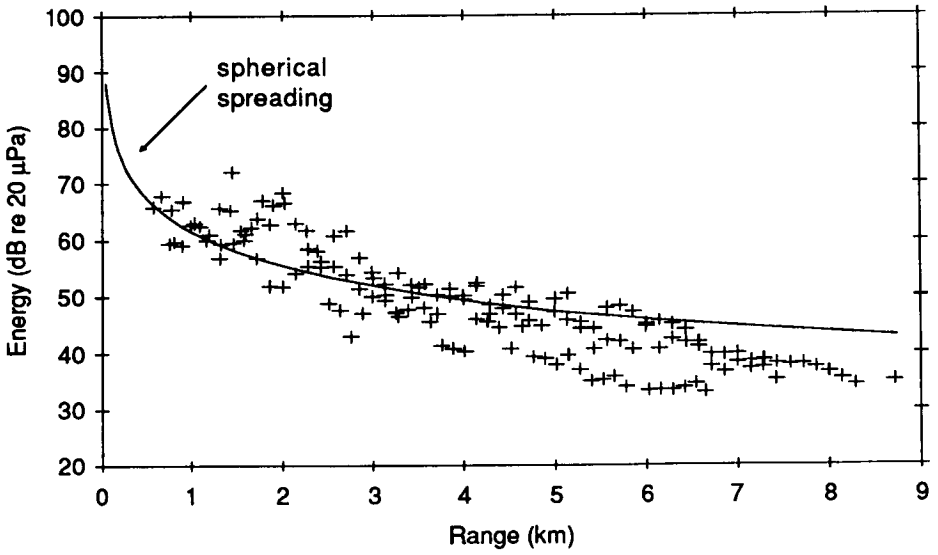

b) experimental data.

Figure 12. Jet outgoing to the North (Day 2).

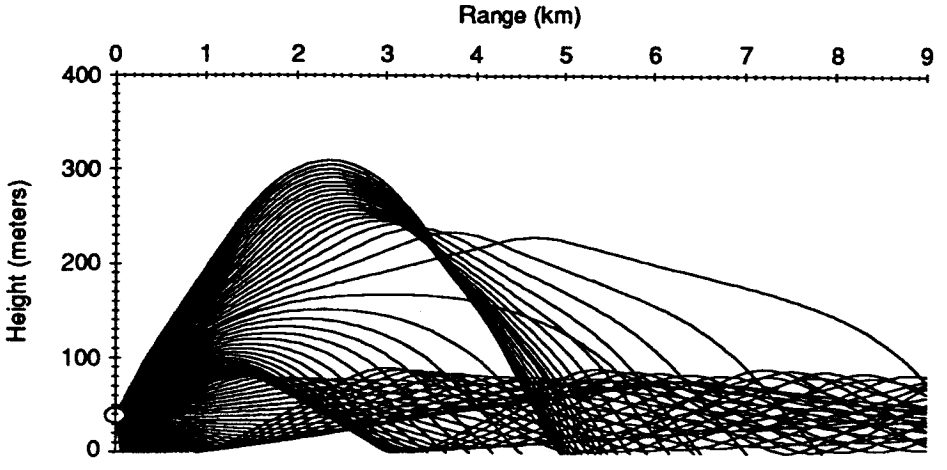

a) raytrace calculated from the velocity profile in Figure 9b.

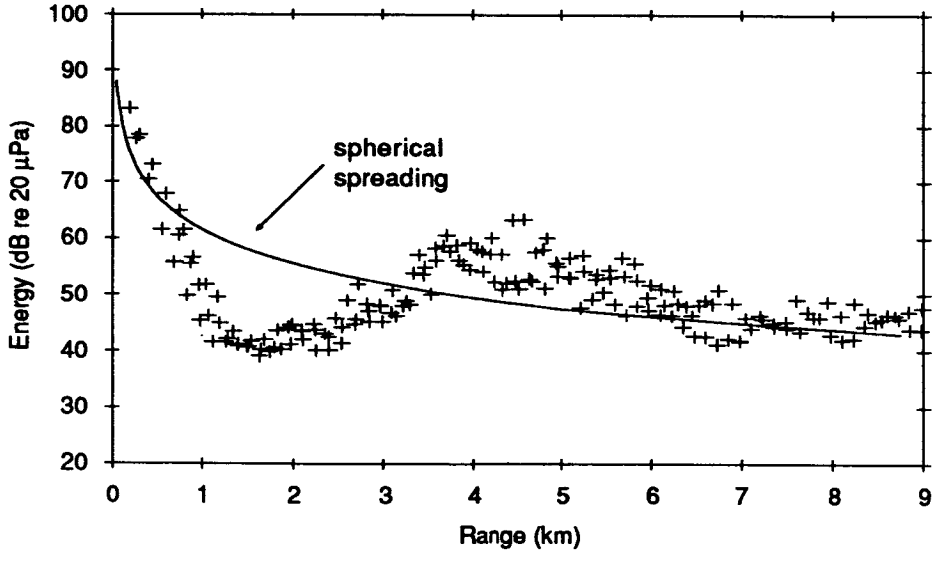

b) experimental data.

Figure 13. Jet outgoing to the South (Day 2).

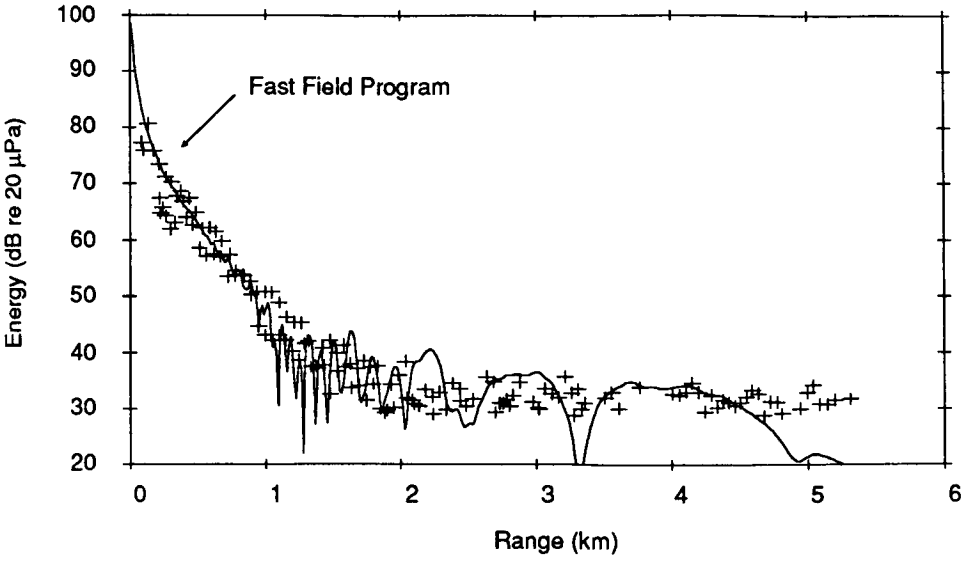

a) helicopter incoming from the North.

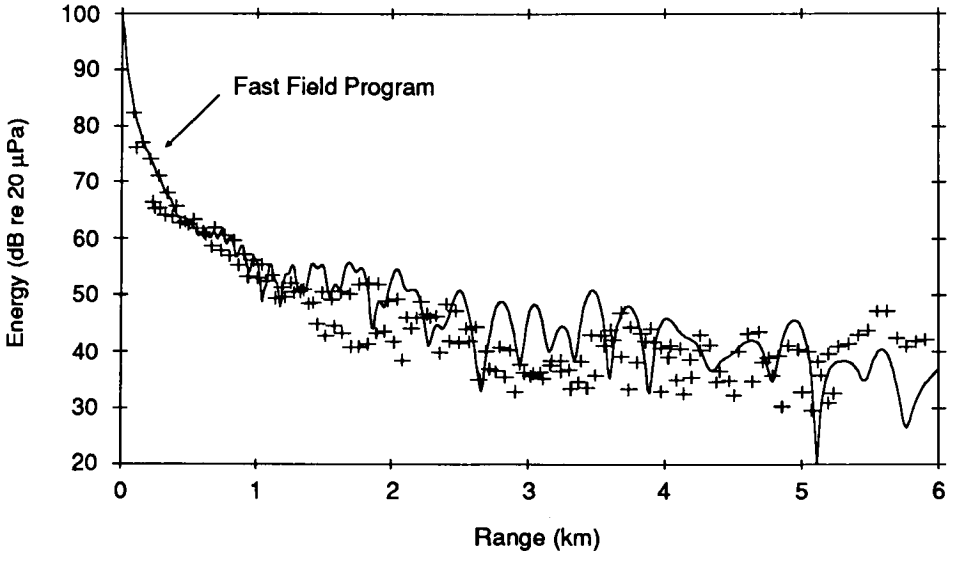

b) helicopter incoming from the South.

Figure 14. Comparison of Day 1 experimental data with the FFP.

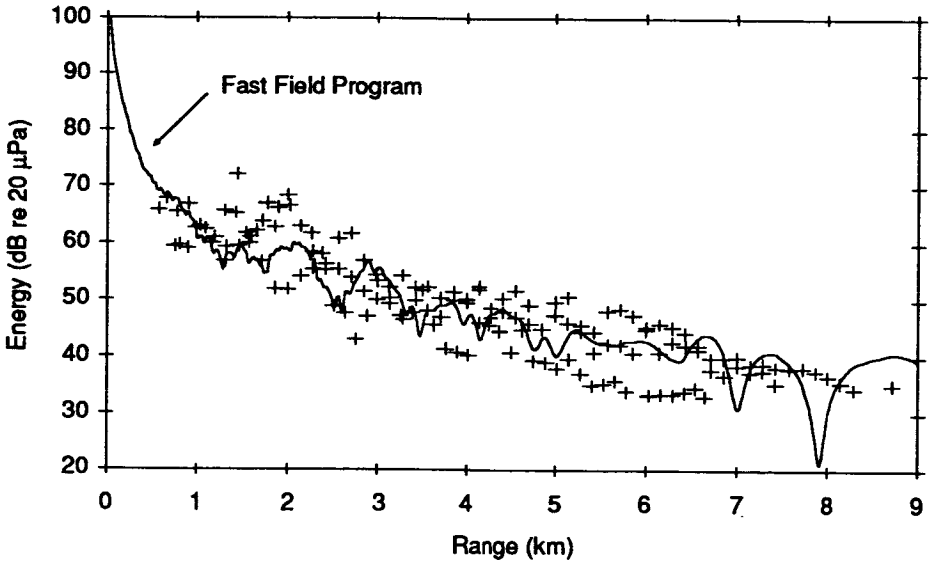

a) jet outgoing to the North.

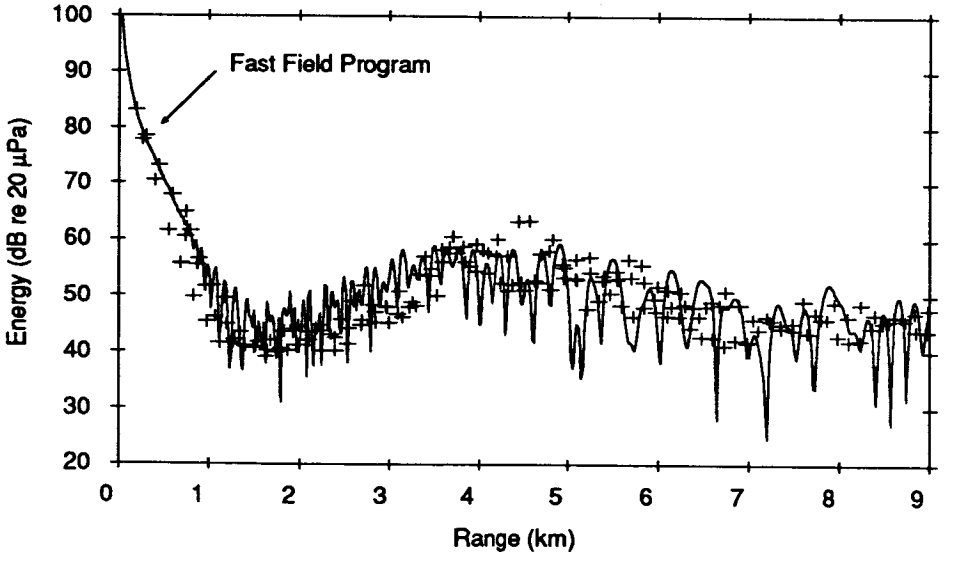

b) jet outgoing to the South.

Figure 15. Comparison of Day 2 experimental data with the FFP.